

Geraniol and Limonene Interaction with 3-hydroxy-3-methylglutaryl-CoA (HMG-CoA) Reductase for their Role as Cancer Chemo-preventive Agents

Madhumita Pattanayak^{1,2}, P K Seth³, Suchi Smita⁴, Shailendra K Gupta^{1,5*}

¹Indian Institute of Toxicology Research, Lucknow (CSIR) India

²Centre for Cellular and Molecular Biology, Hyderabad (CSIR) India

³Biotech Park, Lucknow India

⁴Department of Biological Sciences, University of Rostock, Rostock Germany

⁵System Biology & Bioinformatics Group, University of Rostock, Rostock Germany

Abstract

Recent studies have shown that monoterpenes exhibit antitumor activities and suggest that these compounds are a new class of cancer chemo-preventive agents. Limonene, a main constituent of orange and citrus peel oils has been reported to exert antitumor activity against mammary gland, lung, liver, stomach and skin cancers in rodents whereas, geraniol, a principal constituent of Geranium and Ocimum inhibits the growth of human colon cancer cells. Prenylation of proteins is essential for progression of cells into the S phase and involves post-translational covalent attachment of a lipophilic farnesyl or geranylgeranyl isoprenoid group to numerous proteins. Suppression of prenylation of proteins leads to inhibition of DNA synthesis. Further, epidemiologic evidences suggest that suppression of hydrophilic 3-hydroxy-3-methylglutaryl-CoA (HMG-CoA) reductase, a key enzyme of mevalonate biosynthesis, leads to reduction of the mevalonate pool and thus limits protein isoprenylation.

Geraniol and limonene inhibit the activity of HMG-CoA reductase subsequently reducing the possibility of cancer growth. In the present work, we analyzed binding affinity of limonene and geraniol with HMG-CoA and explored mechanism of interaction using *in silico* approaches. The binding positions were verified according to their energy, PMF (Potential of Mean Force) value, PLP (Piecewise Linear Potential) value and Ligand Internal energy. It was found that limonene had greater binding affinity with the receptor suggesting better antitumor agent in comparison to geraniol.

Keywords: Limonene; Geraniol; HMG CoA reductase; Cancer chemo-preventive agents; docking

Introduction

Essential oils are highly concentrated volatile aromatic essences of plants. They are mainstay of aromatherapy but are also used in flavoring, perfumes and even as solvents. Terpenes, aldehydes, esters, ketones, alcohol, phenol and oxides are major components of essential oils. Monoterpenes function physiologically as chemo-attractants or chemo-repellents, and they are largely responsible for the distinctive fragrance of many

plants (McGrarvey et al., 1995). Significant scientific evidences are there to suggest that nutritive and non-nutritive plant-based dietary factors can inhibit the process of carcinogenesis effectively (Singletary, 2000). Monoterpenes are non nutritive dietary components found in the essential oils of plants having antitumor activity, exhibiting not only the ability to prevent the formation or progression of cancer, but also regress existing malignant tumors (Crowell, 1999). The human exposure to monoterpenes through the diet or environment is widespread.

Major monoterpenes includes limonene, pinenene, menthol, geraniol, camphene, sabinene, cadinine. Monoterpenes consist of two isoprene units with the molecular formula C₁₀H₁₆. Monoterpenes may be linear (acyclic) or contain rings. These 10 carbon isoprenoids are derived from the mevalonate pathway in plants but are not produced by mammals, fungi or other species (Loza-Tavera, 1999). Citrus fruit, orange and peppermint are the main sources of *d*-limonene i.e. *p*-mentha-1,8-diene (Kodama et al., 1977). *d*-limonene (Figure 1) is a prevalent flavoring agent and because of its pleasant citrus fragrance, it is commonly added to cosmetics, soaps and other cleaning products. It is a cyclic monoterpene and formed by the cyclization of geranylpyrophosphate in a reaction catalyzed by *limonene synthase* (Alonso et al., 1992; Kjonas et al., 1983). Limonene has well-established chemo-preventive activity against many cancer types. Limonene has been shown to inhibit the development of spontaneous neoplasms in mice at the dose of 1200 mg/kg orally (National Toxicology Program, 1990). Dietary limonene also reduces the incidence of spontaneous lymphomas in p53^{-/-} mice (Salim et al., 2003). When administered either in pure form or as orange peel oil (95% *d*-limonene), limonene inhibits the development of chemically induced rodent mammary (Asamoto et al., 2002), skin (Elegbede et al., 1986), liver (Lu et al., 2004), lung and stomach (Raphael and Kuttan, 2003) cancers. In rat

***Corresponding author:** Shailendra K Gupta, System Biology & Bioinformatics Group, University of Rostock, 18051, Rostock, Germany, Fax: +49 381 4987572; Tel: +49 381 4987578; E-mail: shailendra.gupta@uni-rostock.de

Received September 26, 2009; **Accepted** November 23, 2009; **Published** November 24, 2009

Citation: Pattanayak M, Seth PK, Smita S, Gupta SK (2009) Geraniol and Limonene Interaction with 3-hydroxy-3-methylglutaryl-CoA (HMG-CoA) Reductase for their Role as Cancer Chemo-preventive Agents. J Proteomics Bioinform 2: 466-474. doi:10.4172/jpb.1000107

Copyright: © 2009 Pattanayak M, et al. This is an open-access article distributed under the terms of the Creative Commons Attribution License, which permits unrestricted use, distribution, and reproduction in any medium, provided the original author and source are credited.

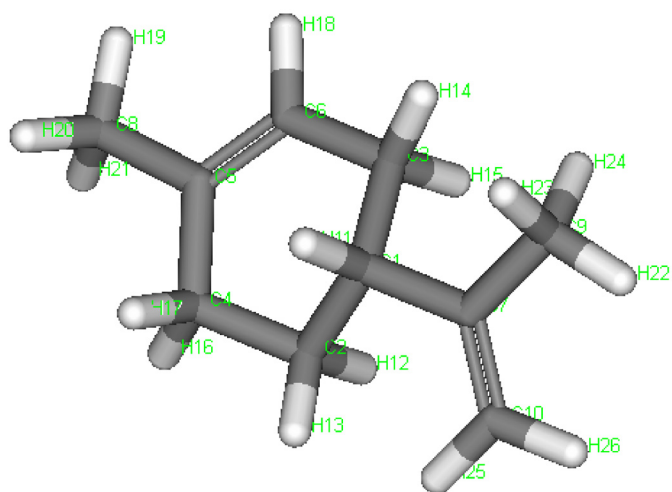


Figure 1: Chemical structure of *d*-limonene (*p*-mentha-1,8-diene).

M.F: C₁₀H₁₆, CAS No: 5989-27-5.

mammary carcinogenesis models, the chemo-preventive effects of limonene are evident during the initiation phase of 7-12-dimethylbenz[*a*]anthracene (DMBA)-induced cancer (Elson et al., 1988) and during the promotion phase of both DMBA- and nitrosomethylurea (NMU)-induced cancers (Chander et al., 1994). Dietary limonene also inhibits the development of *ras* oncogene-induced mammary carcinomas in rats (Gould et al., 1994). Development of azoxymethane-induced aberrant crypt foci in the colon of rats was significantly reduced when they were given 0.5% limonene in the drinking water (Kawamori et al., 1996).

Main sources of geraniol i.e. trans-3,7-Dimethyl-2,6-octadien-1-ol (Figure 2) are bergamot, carrot, coriander, lavender, lemon, lime, nutmeg, orange, rose, blueberry, basil and blackberry. It is mainly used in perfumery and flavouring industries. *Geraniol synthase* is involved in the terpene biosynthetic pathway converting geranyl diphosphate to geraniol (Iijima et al., 2004). Geraniol, an acyclic monoterpene, has antitumor activity against murine leukemia, hepatoma and melanoma cells *in vivo* when administered before and after tumor cell transplantation. It has antiproliferative effects on hepatoma and melanoma cell growth (Polo and de Bravo, 2006). Geraniol (400 μM) caused a 70% inhibition of cell growth in human colon cancer cell lines. Ge-

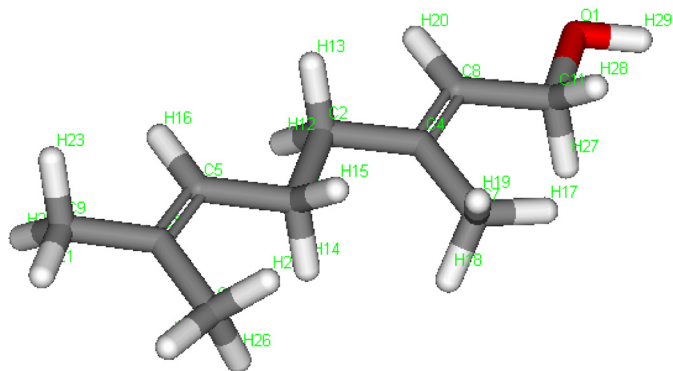


Figure 2: Chemical structure of geraniol (trans-3,7-Dimethyl-2,6-octadien-1-ol).

M.F: C₁₀H₁₈O, CAS No: 106-24-1.

raniol has shown anti-tumoral efficacy on TC-118 human tumors transplanted in Swiss nu/nu mice. Geraniol (150 μM) has been identified to reduce thymidylate synthase and thymidine kinase expression in cancer cells. In nude mice, the combined administration of 5-fluorouracil (20 mg/kg) and geraniol (150 mg/kg) caused a 53% reduction of the tumor volume, whereas a 26% reduction was obtained with geraniol alone (Carnesecchi et al., 2004).

HMG-CoA reductase (Figure 3) is a polytopic, transmembrane protein that catalyzes a key step in the mevalonate pathway (conversion of HMG-CoA to mevalonate). Mevalonate is necessary for cell growth (Swanson and Hohl, 2006) and is involved in the synthesis of sterols, isoprenoids and other lipids. *HMG-CoA reductase* is the rate-limiting step in cholesterol synthesis and represents the sole major drug target for contemporary cholesterol-lowering drugs (Genser et al., 2008). *HMG-CoA reductase* is also an important developmental enzyme. Limonene and

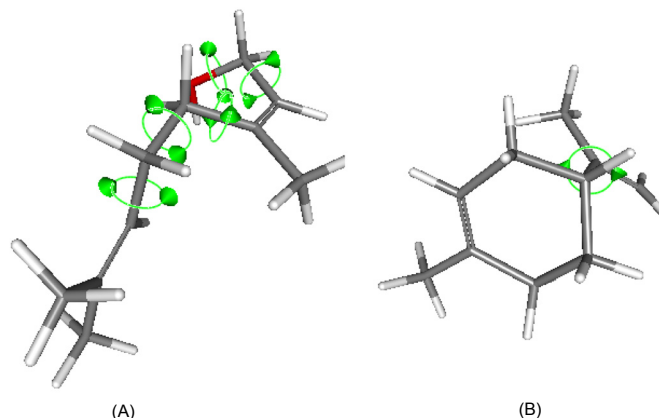


Figure 3: Rotatable bonds shown in green circle (A) Geraniol: with 5 rotatable bonds (B) Limonene: with 1 rotatable bond.

geraniol suppress *HMG-CoA reductase* synthesis in mammalian cells by decreasing the translational efficiency of *HMG-CoA reductase* transcripts (Peffley and Gayen, 2003) and thus reduce mevalonate production. Terpenoids reduce cancer formation by the simple reduction of synthesis of cholesterol and ubiquinone and other cholesterol derivatives that are necessary for the cell proliferation. It is speculated that mevalonate is probably involved in the post-translational modification of proteins involved in cell turnover. The reduction of the mevalonate pool limits protein isoprenylation, which involves the post-translational covalent attachment of a lipophilic farnesyl or geranylgeranyl isoprenoid group to numerous proteins (Clarke, 1992).

Materials and Methods

Preparation of the Receptor and the Ligands

The structure file of *HMG-CoA reductase* complexed with atorvastatin (an inhibitor) was downloaded from Protein Data Bank (PDB id: 1HWK). Structure was resolved using x-ray crystallography experiment at 2.22 Å resolution with R-value 0.212 from *Homo sapiens* (Istvan and Deisenhofer, 2001). To study the interaction of *HMG-CoA reductase* with geraniol and limonene, water molecules and non-protein residues were deleted from the complex. CHARMM forcefield was applied to

study the molecular dynamics. CHARMM uses a flexible and comprehensive empirical energy function that is a summation of many individual energy terms. The energy function is based on separable internal coordinate terms and pairwise nonbond interaction terms (Brooks et al., 1983). The total energy is expressed by equation 1.

$$E = E_b + E_\theta + E_\phi + E_\omega + E_{vdW} + E_{el} + E_{hb} + E_{Cr} + E_{C\phi} \quad (1)$$

where, E is the total energy; E_b (bond potential), E_θ (bond angle potential), E_ϕ (Dihedral angle potential), E_ω (improper torsions) are internal energy terms; E_{vdW} (Van der Waals interactions), E_{el} (Electrostatic potential), E_{hb} (hydrogen bond energy) are nonbonded internal/external interactions energy terms. E_{Cr} (constraints) and $E_{C\phi}$ (user defined energy function) are special energy terms.

Identification of Binding Cavity on Receptor Surface

After energy minimization, the binding pockets of the receptor were determined by using “eraser” algorithm using Accelrys Discovery Studio. This algorithm is first used to remove all grid points outside the receptor. The boundary between the “inside” and “outside” region is determined by the “site opening” parameter. For the remaining grid points (i.e., those “inside” the site), a flood-filling algorithm is employed to find contiguous regions consisting of unoccupied, connected grid points. Each such region is identified as a possible site. A user-specified size cutoff used to remove sites smaller than the specified volume for further consideration (Venkatachalam et al., 2003).

Interaction Protocol and Scoring Functions for Docking

The interaction of the receptor and the ligand was performed using “LigandFit” protocol on Accelrys Discovery Studio. In the first phase of LigandFit docking procedure, binding sites were identified on the receptor surface. Site partitioning approach was followed to sample different parts of the larger binding site for docking. In the second phase, docking between receptor and ligand was performed in the specified site.

Docking ligands to the specified sites has different approaches like conformational search to generate candidate ligand conformations for docking, ligand/site shape matching to select ligand conformations that are similar to the shape of site or site partitions. Candidate ligand poses in the binding site are evaluated and prioritized according to the DockScore function on the basis of forcefield approximation (equation 2), Piecewise Linear Potential function (PLP) (equation 3), LigScore1, LigScore2, Potential of Mean Force (PMF) and Jain scores.

$$\text{DockScore}(\text{forcefield}) = - (\text{ligand/receptor interaction energy} + \text{ligand internal energy}) \quad (2)$$

$$\text{DockScore}(\text{PLP}) = - (\text{PLP potential}) \quad (3)$$

As shown in Eq. 2, this version of DockScore contain two energy terms, these are internal energy of the ligand and the interaction energy of the ligand with the receptor. The interaction energy is taken as the sum of the van der Waals energy and electrostatic energy. To reduce the time needed for the computation of the interaction energy, a grid-based estimation of the ligand/receptor interaction energy is employed. PLP is a fast, simple, docking function that has been shown to correlate well

with protein-ligand binding affinities. PLP scores are measured in arbitrary units, with negative PLP scores reported in order to make them suitable for subsequent use in consensus score calculations. Higher PLP scores indicate stronger receptor-ligand binding (larger pK_i values). *LigScore1* is a scoring function for predicting receptor-ligand binding affinities. *vdW*, *C+pol* and *TotPol*² descriptors are used to calculate *LigScore1* (equation 4, 5), which is computed in units of pK_i ($-\log K_i$). When scoring ligands, the individual contributions of these descriptors may also be provided along with the overall *LigScore1* value. Two slightly different equations are used in the calculation of *LigScore1* depending on the forcefield (Dreiding or CFF) employed for the calculation of the vdW descriptor and the corresponding charge model (Gasteiger or CFF) used to assign atoms as polar or nonpolar.

LigScore2 is another fast and simple scoring function for predicting receptor-ligand binding affinities. *vdW*, *C+pol*, and *BuryPol*² descriptors are used to calculate *LigScore2* (equation 6,7), which is computed in units of pK_i ($-\log K_i$). When scoring ligands, the individual contributions of these descriptors may also be provided along with the overall *LigScore2* value. Two slightly different equations are used in the calculation of *LigScore2* depending on the forcefield (Dreiding or CFF) employed for the calculation of the vdW descriptor.

$$\text{LigScore1_CFF} = 0.4896 - 0.04551 * \text{vdW} + 0.1439 * \text{C+pol} - 0.001010 * \text{TotPol}^2 \quad (4)$$

$$\text{LigScore1_Dreiding} = -0.3498 - 0.04673 * \text{vdW} + 0.1653 * \text{C+pol} - 0.001132 * \text{TotPol}^2 \quad (5)$$

$$\text{LigScore2_CFF} = 1.900 - 0.0730 * \text{vdW} + 0.06246 * \text{C+pol} - 0.00007324 * \text{BuryPol}^2 \quad (6)$$

$$\text{LigScore2_Dreiding} = 1.539 - 0.07622 * \text{vdW} + 0.6501 * \text{C+pol} - 0.00007821 * \text{BuryPol}^2 \quad (7)$$

where the coefficients were obtained through regression analysis of the binding affinities of a series of protein-ligand complexes (Krammer et al., 2005).

The PMF scoring function (Muegge et al., 2005) is based on statistical analysis of the 3D structures of protein-ligand complexes. They were found to correlate well with protein-ligand binding free energies while being fast and simple to calculate. The scores are calculated by summing pairwise interaction terms over all interatomic pairs of the receptor-ligand complex.

The Jain score is a sum of five interaction terms (Jain, 1996). These are Lipophilic interactions, Polar attractive interactions, Polar repulsive interactions, Solvation of the protein and ligand and an entropy term for the ligand. Only proximate protein-ligand atoms are considered for the pairwise interaction terms. The lipophilic and polar interaction terms are each represented by a weighted sum of a Gaussian and a sigmoidal function. This functional form is short-ranged with a pronounced maximum that occurs at close surface contacts. It also incurs a significant penalty for short contacts between protein and ligand atoms.

Parameters for Docking Study

For docking study, the Energy Grid Force Field parameter was set to Dreiding, for computing ligand-protein interaction energy. The Energy Grid parameters control the grid bases dock-

ing used in the initial evaluation of the poses. In the Dreiding force field the Gasteiger charging method is employed to calculate the partial charges of ligands and proteins. The Energy Grid Extension from site was set to 5.0 Å. The Conformation search Number of Monte Carlo Trial was set to "0" to perform a rigid docking. Maximum poses for ligand in the receptor cavity was set to 10. Ligand poses in the receptor cavity were evaluated using LigScore1, LigScore2, PLP1, PLP2, PMF, Jain, Dock Score empirical scoring functions.

Result and Discussion

Molecular properties of geraniol and limonene were analysed, to identify, if they are satisfying Lipinski rule of 5. According to

Lipinski rule of 5, for any druggable compound, molecular weight should be less than 500; number of H-donors less than 5; number of H-acceptor less than 10; and octanol-water partition coefficient (ALogP) value should be less than 5. Calculated molecular properties values of geraniol and limonene are shown in Table 1. Rotatable bonds of geraniol and limonene are shown in Figure 3. Geraniol contains total 5 rotatable bonds, while limonene has only 1 rotatable bond. Ligand conformations were generated using search small molecule confirmation tools available in Accelrys discovery studio. Systematic search method was used with energy threshold 20 kcal/mol to generate total 56 conformation poses of geraniol (Table 2). Energy plot of all 56 confirmation poses of geraniol is shown in Figure 4. In

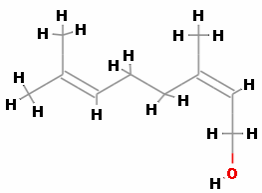
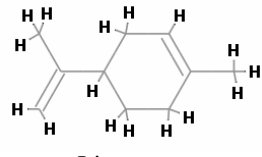
Ligand	Mol. Formula	Mol. Weight	No. of H_Acceptors	No. of H_donors	AlogP	No. of Rotatable Bonds
 Geraniol	C ₁₀ H ₁₈ O	154.249	1	1	2.934	5
 Limonene	C ₁₀ H ₁₆	136.234	0	0	3.502	1

Table 1: Molecular properties of Geraniol and Limonene.

Confirmation index	Angle 1	Angle 2	Angle 3	Angle 4	Angle 5	Relative Energy	Energy
0	178.238	288.239	343.105	304.69	301.204	7.44572	50.0316
1	179.262	168.06	342.579	304.651	301.937	7.96441	50.5503
2	178.916	286.762	104.3	305.295	299.859	1.93152	44.5174
3	178.128	167.4	104.412	305.207	299.881	1.60827	44.1941
4	60.6897	171.495	100.998	304.873	300.957	18.4569	61.0428
5	178.176	288.753	343.164	65.0501	300.378	5.50335	48.0892
6	179.093	167.801	342.991	66.3717	298.548	7.02377	49.6096
7	180.618	165.701	101.815	69.0623	299.17	18.9884	61.5743
8	181.456	44.8951	225.639	61.0061	303.736	15.073	57.6589
9	174.811	170.853	227.034	60.0737	304.949	15.066	57.6519
10	178.19	288.769	343.133	185.549	299.275	4.57314	47.159
11	179.119	167.91	342.856	185.862	298.753	6.00858	48.5944
12	178.899	286.839	104.229	185.361	299.33	0.369732	42.9556
13	295.353	292.389	98.4318	185.164	298.612	17.8395	60.4254
14	178.18	167.447	104.337	185.311	299.288	0.018356	42.6042
15	60.8582	171.667	100.883	184.951	298.309	16.8683	59.4542
16	182.279	43.9313	226.301	187.387	295.475	14.6417	57.2276
17	175.09	170.56	226.68	187.671	295.75	12.1075	54.6933
18	177.996	289.147	342.882	303.963	60.7323	17.6641	60.25
19	179.726	168.673	341.645	303.091	62.4863	16.1245	58.7103

20	178.675	287.051	104.57	303.021	62.2214	6.34724	48.9331
21	177.67	167.226	105.03	302.726	62.3295	5.92371	48.5096
22	178.187	288.763	343.142	64.0312	61.7222	4.63044	47.2163
23	179.108	167.848	342.915	65.0618	60.3784	6.30299	48.8888
24	177.059	291.348	101.869	70.372	44.1838	5.65112	48.237
25	179.766	166.912	102.457	69.9686	44.437	6.75359	49.3394
26	181.38	44.9906	225.574	60.0213	64.1675	13.5505	56.1364
27	174.744	170.753	227.108	58.4664	65.7236	13.7757	56.3616
28	178.19	288.769	343.133	184.843	60.5746	4.59975	47.1856
29	179.116	167.893	342.888	184.768	60.724	6.05384	48.6397
30	178.899	286.839	104.229	184.634	60.6536	0.340797	42.9266
31	295.359	292.377	98.4477	183.873	61.2033	17.8911	60.477
32	178.18	167.447	104.337	184.556	60.6654	0.001579	42.5874
33	60.8537	171.675	100.891	183.4	61.4292	16.9265	59.5124
34	182.364	43.8285	226.388	186.164	57.409	14.6264	57.2122
35	175.097	170.568	226.685	186.514	57.8005	11.7829	54.3688
36	178.17	288.82	343.087	304.695	178.643	6.55064	49.1365
37	179.264	168.071	342.557	303.874	178.702	8.04005	50.6259
38	178.916	286.762	104.3	304.676	178.553	2.00141	44.5873
39	178.128	167.4	104.412	304.564	178.525	1.67498	44.2608
40	60.6915	171.399	101.035	303.869	176.535	18.5049	61.0908
41	184.126	46.0999	225.24	287.926	143.951	14.745	57.3308
42	178.187	288.763	343.143	64.6461	181.316	4.5938	47.1796
43	179.106	167.838	342.936	65.7858	180.442	6.27443	48.8603
44	177.06	291.342	101.883	71.7591	190.121	6.68425	49.2701
45	178.347	167.413	104.03	67.0523	185.102	8.86106	51.4469
46	181.431	44.9197	225.631	60.595	183.6	13.7376	56.3234
47	174.747	170.761	227.115	59.3521	185.007	13.8229	56.4087
48	178.19	288.769	343.133	185.193	180.07	4.55102	47.1369
49	179.118	167.904	342.871	185.353	180.094	5.99049	48.5763
50	178.899	286.839	104.229	184.995	180.111	0.348484	42.9343
51	295.331	292.407	98.4122	184.587	180.408	17.7122	60.298
52	178.18	167.447	104.337	184.931	180.104	0	42.5858
53	60.8559	171.59	100.926	184.26	180.46	16.7734	59.3593
54	182.413	43.7613	226.427	186.802	176.185	14.7068	57.2927
55	175.099	170.567	226.675	187.084	176.559	11.7129	54.2988

Table 2: Confirmation poses of Geraniol generated using systematic search with energy threshold 20 kcal/mol.

Confirmation index	Angle 1	Relative Energy	Energy
0	144.977	0	42.4817
1	264.12	5.57912	48.0608
2	24.1618	15.9883	58.47

Table 3: Confirmation poses of Limonene generated using systematic search with energy threshold 20 kcal/mol.

limonene, only 1 rotatable bond was present, thus only 3 conformation poses were generated using systematic search conformation generation method at energy threshold 20 kcal/mol (Table 3). Energy plot of all 3 confirmation poses of limonene is shown in Figure 5. *HMG-CoA reductase* chain A was analysed for all the possible binding sites (Figure 6). These active sites were selected from the receptor according to their volume of the binding cavity. Docking was performed by selecting one site at a time. Binding site 2 with 326 interacting points and 40.750 Å³ volume showed interaction with both geraniol and

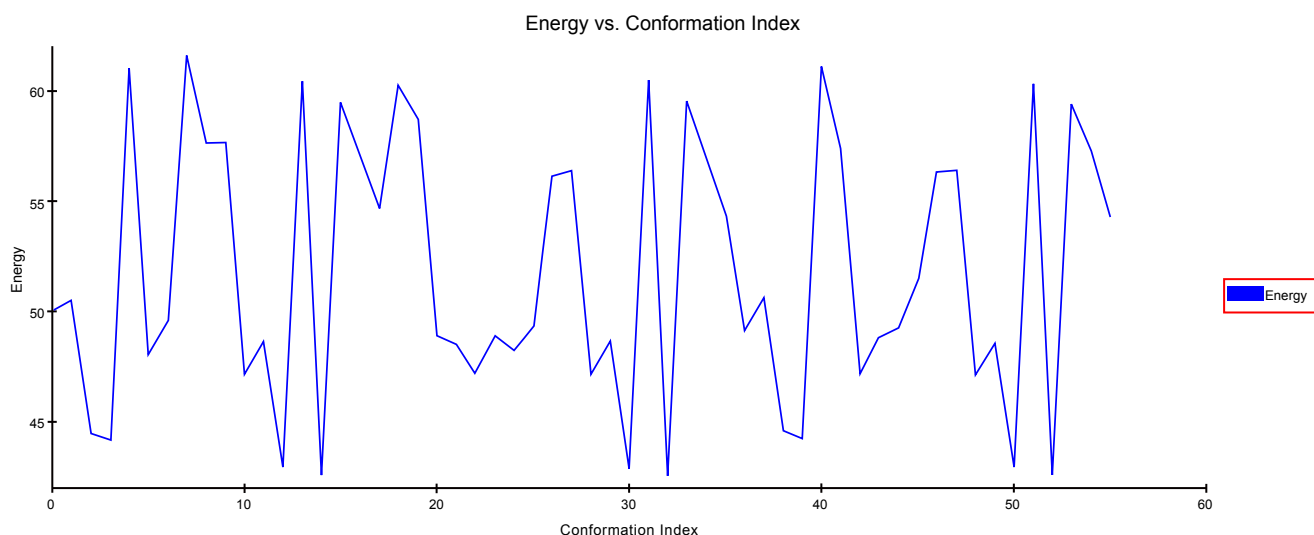


Figure 4: Energy plot of all 56 confirmation poses of Geraniol.

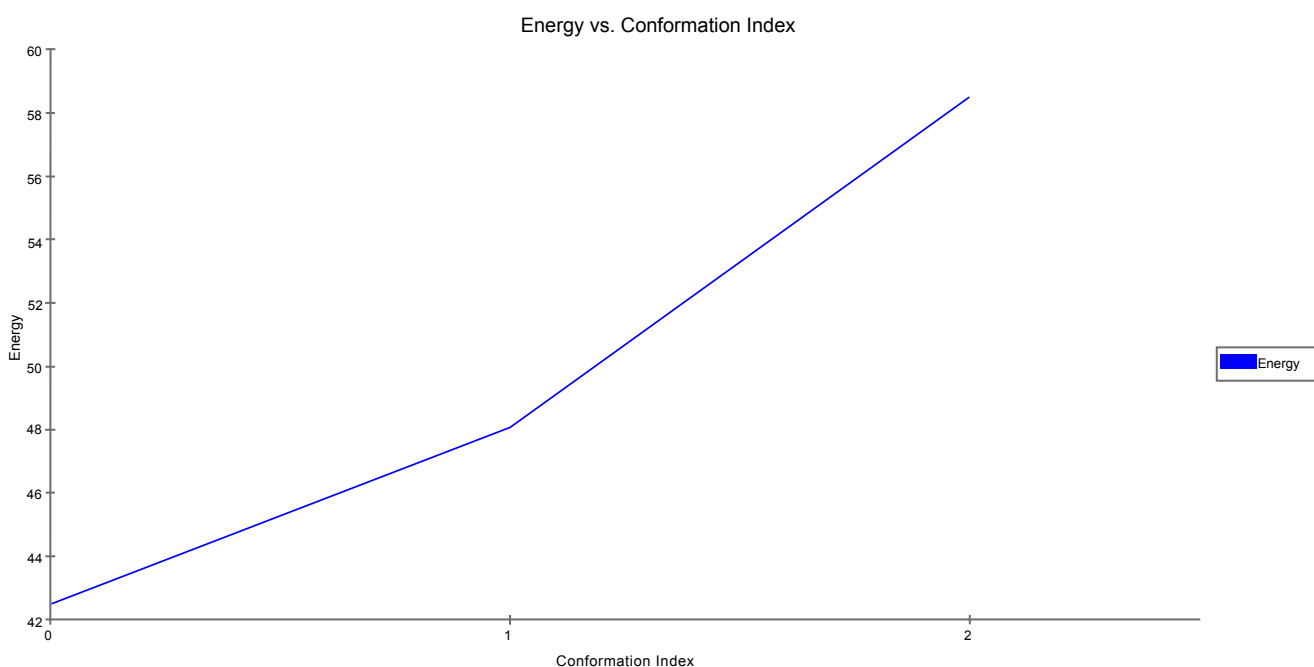


Figure 5: Energy plot of all 3 confirmation poses of Limonene.

limonene (Figure 7). Best poses for each geraniol and limonene with *HMG-CoA reductase* were analysed for different energy parameters.

***HMG-CoA reductase* -geraniol Interaction**

Docking was performed with all 56 conformation poses of geraniol and top 8 poses were analysed in the binding cavity of *HMG-CoA reductase* (Table 4). The best pose of geraniol (with dock score = 9.448) interacting with threonine 809, aspartic acid 767 and glycine 765 of *HMG-CoA reductase*. The hydrogen atom at position 29 of geraniol interacts with hydrogen atom at position 22 of threonine present at position 809 of *HMG-CoA reductase*. Same hydrogen atom at position 29 of geraniol interacts with oxygen of the C=O of glycine present at position 765 of the receptor molecule. Hydrogen at position 20 of geraniol

interacts with hydrogen beta 1 of aspartic acid at position 767. Total ligand internal energy for the best post is calculated to 7.642. (Figure 8).

***HMG-CoA reductase* -limonene Interaction**

For limonene and *HMG-CoA reductase* interaction, we generated three conformations using small molecule conformation generation method. All three poses of limonene were analyzed in the binding cavity of *HMG-CoA reductase*. The best pose of limonene has dock score as high as 10.593, much more than the best dock score in case of geraniol (Table 4). Best pose of limonene has three atoms interacting with *HMG-CoA reductase*. These are hydrogen at position 20, 17 and carbon at position 3. Hydrogen at position 20 and carbon at position 3 form bond with hydrogen atom of glycine amino ter-

Ligand	Conformation pose	LigScore1	LigScore2	-PLP1	-PLP2	Jain	-PMF	Dock Score
Geraniol	1	0.86	2.72	45.43	46.43	0.46	-7.24	9.448
	2	0.7	2.48	31.06	32.85	-0.28	-4.61	8.023
	3	0.77	2.57	30.55	32.64	-0.26	-4.77	7.93
	4	0.55	2.47	44.12	47.07	1.55	-11.37	5.818
	5	0.54	2.47	44.43	47.28	1.48	-11.1	5.805
	6	0.55	2.48	44.48	47.14	1.56	-10.45	5.786
	7	0.07	2.09	40.79	41.66	-0.25	-7.02	5.202
	8	0.23	2.29	51.9	53	1.05	-4.42	3.424
Limonene	1	0.32	2.6	26.07	25.32	-0.52	8.56	15.035
	2	0.03	2	25.88	28.97	1.67	-7.25	10.593
	3	-0.55	1.09	32.31	36.06	1.3	-15.66	0.736

Table 4: Conformation poses of geraniol and limonene with different scoring functions. Poses are arranged with the descending dock score value.

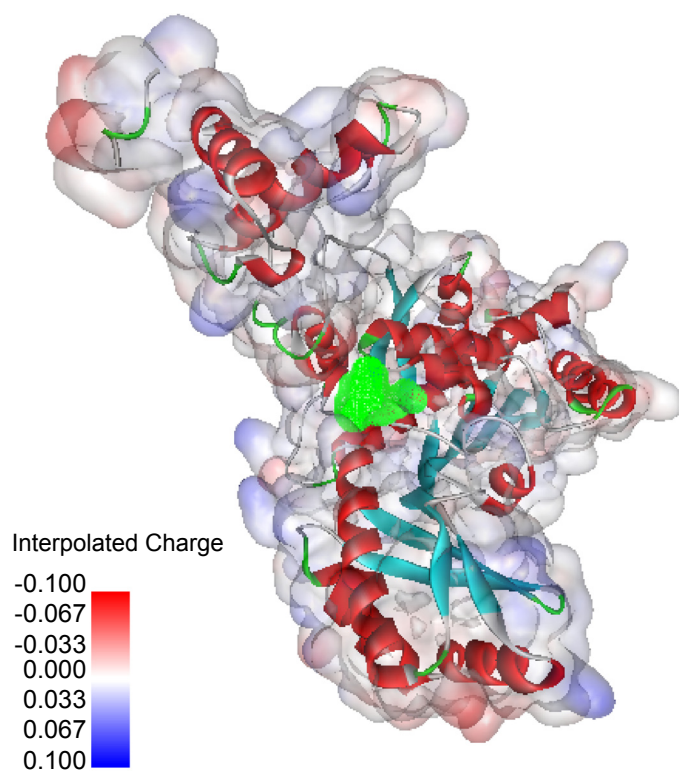


Figure 6: 3-hydroxy-3-methylglutaryl-CoA (HMG-CoA) reductase (chain A). Molecular surface is colored based on calculated interpolated charges. Protein back bone is displayed as solid ribbon and colored by secondary structure type. Binding site 2 is shown with green dots.

minus at position 808. The second interaction is in between hydrogen at position 17 of limonene and H- β 1 of aspartic acid present at position 767 of *HMG-CoA reductase* (Figure 9).

Conclusion

Molecular docking studies provide lead to determine the potential of ligand interaction in the binding cavities of receptor molecules. Considering the high dock score and low ligand internal energy, it can be concluded that limonene has greater bind-

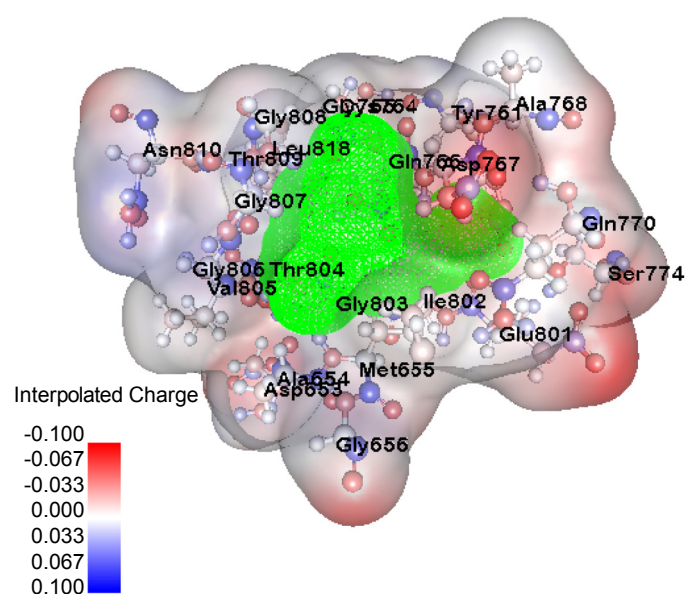


Figure 7: Detail view of binding site in 3-hydroxy-3-methylglutaryl-CoA (HMG-CoA) reductase (chain A). All amino acids, surrounding the binding sites are labeled. Surface is colored based on calculated interpolated charges.

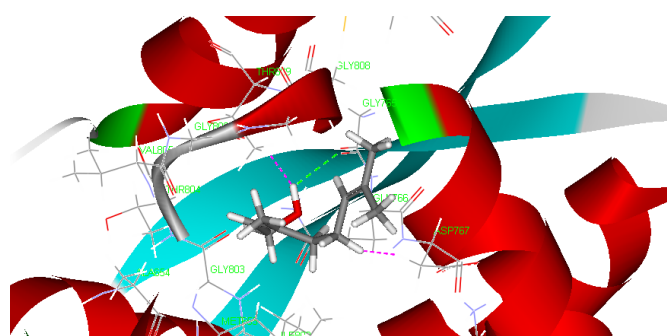


Figure 8: Geraniol interaction with HMG-CoA reductase. All interacting amino acids with the ligand are labeled.

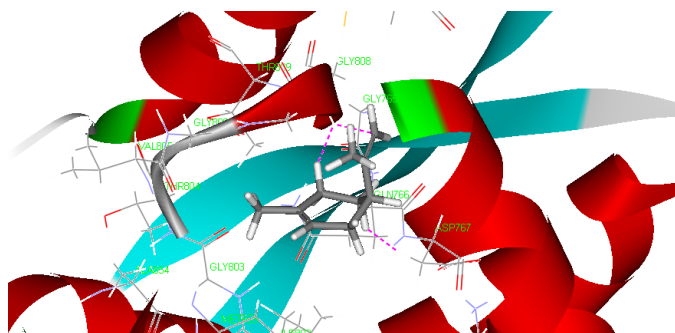


Figure 9: Limonene interaction with HMG-CoA reductase. All interacting amino acids with the ligand are labeled.

ing affinity with *HMG-CoA reductase* and thus having better antitumor activity in comparison to geraniol. Aspartic acid at position 767 of *HMG-CoA reductase* is interacting with both geraniol and limonene. This amino acid acts as a major anchor point for the ligands to interact with the receptor molecule for their anti-tumor activities.

Acknowledgements

SKG acknowledge Director, IITR, Lucknow for his generous support and CSIR NWP-17 project for providing necessary infrastructure for the work.

References

- Alonso WR, Rajaonarivony JI, Gershenzon J, Croteau R (1992) Purification of 4S-limonene synthase, a monoterpene cyclase from the glandular trichomes of peppermint (*Mentha x piperita*) and spearmint (*Mentha spicata*). *J Biol Chem* 267: 7582-7. » [CrossRef](#) » [Pubmed](#) » [Google Scholar](#)
- Asamoto M, Ota T, Toriyama-Baba H, Hokaiwado N, Naito A, et al. (2002) Mammary carcinomas induced in human c-Ha-ras proto-oncogene transgenic rats are estrogen-independent, but responsive to d-limonene treatment. *Jpn J Cancer Res* 93: 32-5. » [CrossRef](#) » [Pubmed](#) » [Google Scholar](#)
- Brooks BR, Bruccoleri RE, Olafson BD, States DJ, Swaminathan S, et al. (1983) CHARMM: A program for macromolecular energy minimization and dynamics calculations. *J Comput Chem* 4: 187-217. » [CrossRef](#) » [Pubmed](#)
- Carnesecchi S, Bras-Gonçalves R, Bradaia A, Zeisel M, Gossé F, et al. (2004) Geraniol, a component of plant essential oils, modulates DNA synthesis and potentiates 5-fluorouracil efficacy on human colon tumor xenografts. *Cancer Lett* 215: 53-9. » [CrossRef](#) » [Pubmed](#) » [Google Scholar](#)
- Chander SK, Lansdown AG, Luqmani YA, Gomm JJ, Coope RC, et al. (1994) Effectiveness of combined limonene and 4-hydroxyandrostenedione in the treatment of NMU-induced rat mammary tumours. *Br J Cancer* 69: 879-82. » [CrossRef](#) » [Pubmed](#)
- Clarke S (1992) Protein isoprenylation and methylation at carboxyl-terminal cysteine residues. *Annu Rev Biochem* 61: 355-86. » [CrossRef](#) » [Pubmed](#) » [Google Scholar](#)
- Crowell PL (1999) Prevention and therapy of cancer by dietary monoterpenes. *J Nutr* 129: 775S-778S. » [CrossRef](#) » [Pubmed](#) » [Google Scholar](#)
- Elegbede JA, Maltzman TH, Verma AK, Tanner MA, Elson CE, et al. (1986) Mouse skin tumor promoting activity of orange peel oil and d-limonene: a re-evaluation. *Carcinogenesis* 7: 2047-9. » [CrossRef](#) » [Pubmed](#) » [Google Scholar](#)
- Elson CE, Maltzman TH, Boston JL, Tanner MA, Gould MN (1988) Anti-carcinogenic activity of d-limonene during the initiation and promotion/progression stages of DMBA-induced rat mammary carcinogenesis. *Carcinogenesis* 9: 331-2. » [CrossRef](#) » [Pubmed](#) » [Google Scholar](#)
- Genser B, Grammer TB, Stojakovic T, Siekmeier R, März W (2008) Effect of HMG CoA reductase inhibitors on low-density lipoprotein cholesterol and C-reactive protein: systematic review and meta-analysis. *Int J Clin Pharmacol Ther* 46: 497-510. » [Pubmed](#) » [Google Scholar](#)
- Gould MN, Moore CJ, Zhang R, Wang B, Kennan WS, et al. (1994) Limonene chemoprevention of mammary carcinoma induction following direct in situ transfer of v-Ha-ras. *Cancer Res* 54: 3540-3543. » [CrossRef](#) » [Pubmed](#) » [Google Scholar](#)
- Iijima Y, Davidovich-Rikanati R, Fridman E, Gang DR, Bar E, et al. (2004) The Biochemical and molecular basis for the divergent patterns in the biosynthesis of terpenes and phenylpropenes in the peltate glands of three cultivars of Basil. *Plant Physiol* 136: 3724-3736. » [CrossRef](#) » [Pubmed](#) » [Google Scholar](#)
- Istvan ES, Deisenhofer J (2001) Structural mechanism for statin inhibition of HMG-CoA reductase. *Science* 292: 1160-4. » [CrossRef](#) » [Pubmed](#) » [Google Scholar](#)
- Jain AN (1996) Scoring noncovalent protein-ligand interactions: a continuous differentiable function tuned to compute binding affinities. *J Comput Aided Mol Des* 10: 427-40. » [CrossRef](#) » [Pubmed](#) » [Google Scholar](#)
- Kawamori T, Tanaka T, Hirose Y, Ohnishi M, Mori H (1996) Inhibitory effects of d-limonene on the development of colonic aberrant crypt foci induced by azoxymethane in F344 rats. *Carcinogenesis* 17: 369-372. » [CrossRef](#) » [Pubmed](#) » [Google Scholar](#)
- Kjonaas R, Croteau R (1983) Demonstration that limonene is the first cyclic intermediate in the biosynthesis of oxygenated p-menthane monoterpenes in *Mentha Piperita* and other *Mentha* species. *Arch Biochem Biophys* 220: 79-89. » [CrossRef](#) » [Pubmed](#) » [Google Scholar](#)
- Kodama R, Yano T, Furukawa K, Noda K, Ide H (1976) Studies on the metabolism of d-limonene (p-mentha-1,8-diene). IV. Isolation and characterization of new metabolites and species differences in metabolism. *Xenobiotica* 6: 377-89. » [CrossRef](#) » [Pubmed](#) » [Google Scholar](#)
- Krammer A, Kirchhoff PD, Jiang X, Venkatachalam CM, Waldman M (2005) LigScore: a novel scoring function for predicting binding affinities. *J Mol Graph Model* 23: 395-407. » [CrossRef](#) » [Pubmed](#) » [Google Scholar](#)
- Loza-Tavera H (1999) Monoterpenes in essential oils. *Bio-synthesis and properties*. *Adv Exp Med Biol* 464: 49-62. » [Pubmed](#) » [Google Scholar](#)
- Lu XG, Zhan LB, Feng BA, Qu MY, Yu LH, et al. (2004) Inhibition of growth and metastasis of human gastric cancer implanted in nude mice by d-limonene. *World J Gastroenterol* 10: 2140-4. » [CrossRef](#) » [Pubmed](#) » [Google Scholar](#)

21. McGarvey DJ, Croteau R (1995) Terpenoid metabolism. *Plant Cell* 7: 1015-1026. » [CrossRef](#) » [Pubmed](#) » [Google Scholar](#)
22. Muegge I, Martin YC (1999) A general and fast scoring function for protein-ligand interactions: a simplified potential approach. *J Med Chem* 42: 791-804.» [CrossRef](#) » [Pubmed](#) » [Google Scholar](#)
23. National Toxicology Program (1990) NTP Toxicology and Carcinogenesis Studies of d-Limonene (CAS No. 5989-27-5) in F344/N Rats and B6C3F1 Mice (Gavage Studies). *Natl Toxicol Program Tech Rep Ser* 347: 1-165.» [Pubmed](#)
24. Peffley DM, Gayen AK (2003) Plant-derived monoterpenes suppress hamster kidney cell 3-hydroxy-3-methylglutaryl coenzyme a reductase synthesis at the post-transcriptional level. *J Nutr* 133: 38-44. » [CrossRef](#) » [Pubmed](#) » [Google Scholar](#)
25. Polo MP, de Bravo MG (2006) Effect of geraniol on fatty-acid and mevalonate metabolism in the human hepatoma cell line Hep G2. *Biochem Cell Biol* 84: 102-11. » [CrossRef](#) » [Pubmed](#) » [Google Scholar](#)
26. Raphael TJ, Kuttan G (2003) Effect of naturally occurring monoterpenes carvone, limonene and perillic acid in the inhibition of experimental lung metastasis induced by B16F-10 melanoma cells. *J Exp Clin Cancer Res* 22: 419-24. » [Pubmed](#) » [Google Scholar](#)
27. Salim EI, Wanibuchi H, Morimura K, Wei M, Mitsuhashi M, et al. (2003) Carcinogenicity of dimethylarsinic acid in p53 heterozygous knockout and wild-type C57BL/6J mice. *Carcinogenesis* 24: 335-42. » [CrossRef](#) » [Pubmed](#) » [Google Scholar](#)
28. Singletary K (2000) Diet, natural products and cancer chemoprevention. *J Nutr* 130: 465S-466S. » [CrossRef](#) » [Pubmed](#) » [Google Scholar](#)
29. Swanson KM, Hohl RJ (2006) Anti-cancer therapy: targeting the mevalonate pathway. *Curr Cancer Drug Targets* 6: 15-37. » [CrossRef](#) » [Pubmed](#) » [Google Scholar](#)
30. Venkatachalam CM, Jiang X, Oldfield T, Waldman M (2003) LigandFit: a novel method for the shape-directed rapid docking of ligands to protein active sites. *J Mol Graph Model* 21: 289-307. » [CrossRef](#) » [Pubmed](#) » [Google Scholar](#)